Studia Geotechnica et Mechanica, Vol. XXXI, No. 1, 2009

ESTIMATION OF INTERNAL FORCES IN THE SHELL OF SOIL-STEEL STRUCTURES ON THE BASIS OF ITS DISPLACEMENTS DURING BACKFILLING

CZESŁAW MACHELSKI

Bridge Division, Civil Engineering Institute, Wrocław University of Technology,
Wybrzeże Wyspiańskiego 27, 50-370 Wrocław, Poland.
Phone: (+48) 71 320-2756, e-mail: czeslaw.machelski@pwr.wroc.pl

Abstract: In the soil-steel structures one can consider two independent states at which the carrying capacity of the steel shell structure reaches its maximum value, i.e., the stage of construction during backfilling and the stage of maximum loading of bridge during proof tests or its service life. Most often, the deformations of arch-shaped steel shells are most dangerous and adverse during the backfilling stage. The process of modelling, by means of FEM-based software, of soil-steel structures during their assembly stages is very complex. Currently, computation results obtained with the help of FEM are not fully satisfactory. A different approach to the estimation of deformation of a steel shell which is effective as well as accurate because of being based on the measurement results of real structures is presented in the paper. Examples of analysis indicate the feasibility of an algorithm derived also for the estimation of internal forces and soil–shell interactions in arch-shaped soil-steel shell bridges and culverts. Calculations can concern construction stages or finished structure, after any service period.

Streszczenie: W konstrukcjach gruntowo-powłokowych wyróżnia się dwa niezależne stany, w których występują największe wytężenia powłoki, tj. faza budowy, czyli układania zasypki oraz maksymalnego obciążenia gotowego mostu podczas jego badań odbiorczych lub eksploatacji. Najczęściej deformacje powłok o kształcie łukowym są najbardziej niekorzystne w fazie zasypki. Modelowanie obiektu guntowo-powłokowego w procesie formowania konstrukcji z użyciem ogólnych systemów MES jest bardzo utrudnione. Wyniki obliczeń z zastosowaniem MES nie są obecnie zadowalające. Odmienne podejście do określania deformacji powłoki, skuteczne i równocześnie dokładne, bo oparte na wynikach pomiarów na budowanych obiektach prezentowane jest w niniejszej pracy. Przykłady analiz wskazują na przydatność algorytmu również do szacowania sił wewnętrznych i oddziaływania gruntu w powłokach mostów gruntowo-powłokowych. Obliczenia mogą dotyczyć fazy budowy lub konstrukcji gotowej, po wybranym okresie jej eksploatacji.

Резюме: В грунтово-оболочных конструкциях выделяются два независимых состояния, в которых выступают предельные натяжения оболочки, т.е. стадии стройки, значит укладывания заполнителя, а также максимальной нагрузки готового моста во время его приемных исследований или разработок. Чаще всех деформации оболочек арочной формы наиболее часто невыгодны в стадии заполнения. Моделирование грунтово-оболочного объекта в процессе формирования конструкции с употреблением общих систем МЭС является очень сложным. Результаты расчетов с применением МЭС в настоящее время неудовлетворительны. В настоящей работе показан другой подход к определению деформации оболочки, который является эффективным и одновременно точным, так как базирует на результатах измерений на строеных объектах. Примеры анализов показывают пригодность алгоритма также для оценки внутренних сил и воздействия грунта в оболочках грунтово-оболочных мостов. Расчеты могут касаться стадии строения или готовой конструкции, после избранного периода ее эксплуатации.

1. INTRODUCTION

The paper concerns the soil-steel circular arch-shaped structures made of the steel corrugated plates. In the design calculations, usually two distinctive states are analyzed, at which the shell can reach its maximum strength, i.e., construction stage which is the backfilling process and the stage of maximum loading that can occur during the service life of a bridge. Both stages can be treated separately and independently, only from the point of view of the change of strains and internal forces in a shell but not with regard to its carrying capacity. This is due to the fact that during its service life the results from external loading, i.e., from traffic load are added to the internal forces, which are derived from the dead load, i.e., the weight of structure. The most dangerous case for the deformation of shells of such structures occurs during backfilling and compaction of backsoil around the steel shell. The displacements during the proof loading (with the maximum burden of loading vehicles) are often several times smaller than during these backfilling processes.

The process of modelling the behaviour of soil-steel structures during their construction stage with the help of FE Method is very complex. Due to the fact that the fundamental elements of soil-steel structure are corrugated plate and surrounding backsoil, each single element must be described by a group of independent parameters such as the module of deformation, Poisson's coefficient and the volume weight [1], [2], [4], [7], [10]. In the case of soil medium treated as the loose body, precise determination of the values of those parameters is a very tough issue because after finishing consecutive layers, compacting devices cause a change of physical characteristics of soil which has been compacted before. Endometric compression module is different with regard to its value for each single compaction layer, even for homogeneous soil. Only the application of elastic-plastic model of the soil and professional FEM-based software enables us to obtain satisfactory results [11]. In the case of finished structure which is subject to static load, the results of calculations made on the basis of the soil elastic model are similar to measurement results, e.g., [1], [6]–[8], [10].

A different approach for the determination of deformation of a structure and internal forces which is more effective and accurate because of being based on the real measurements of displacements of the shell structure with the use of geodetic technique is presented in the paper. Calculation algorithm is intended for the estimation of internal forces derived in the shell in the in-situ construction conditions when the irregular deformation of shell occurs, e.g., unsymmetrical when symmetrical layers of backfilling, ineffective supports of a shell, e.g., the suspension phenomenon of a shell in backsoil. The deformation of the shell estimated on the basis of displacements and linearly elastic material of the shell enables the internal forces to be calculated. In the model proposed, there in no need to take into consideration the material of backsoil, its physical parameters and technology of compaction because in the measured displacements of the shell these are obviously already included. It is the crucial simplification of the calculation process.

The determination of displacements with the help of geodetic technique is much simpler and at the same time more effective than professional measurement technique. The results of geodetic measurements made during construction period can also be used after a lot of years of service.

2. DEFORMATION OF STEEL SHELL DURING BACKFILIING

In the initial stage of backfilling, when the depth of backsoil increases, the forces between soil and shell described by $p(\varphi)$ as in figure 1 are subject to change. They are reduced by the deformation of a flexible shell. When the backsoil is at the level of the arch's top, the reverse deformation of a shell occurs, but there is still an increase in the reaction of the shell on the soil. The tangent forces on the contact surface of a steel shell and soil designated by $t(\varphi)$ are of minor significance at this stage.

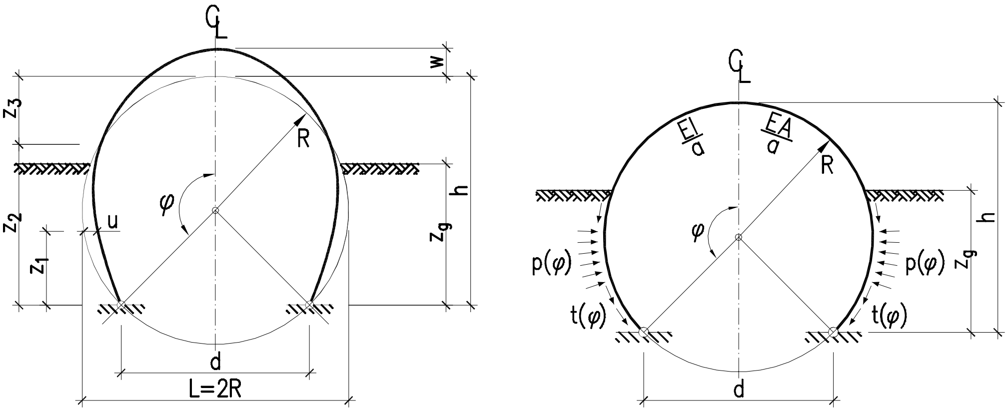

Fig. 1. Plot of the deformation of the shell and the soil–shell interaction forces

The phenomenon of deformation of steel arch-shaped shell during backfilling can be represented by two characteristic displacements, as shown in figure 1, which are the deflections of shell upward, called further in the paper as the rise w, and the change of horizontal, the largest dimension of shell called the narrowing u. The ratios of these displacements at the stage of backfilling are subject to specific changes. The final deformation of a shell, after construction of the road surface depends on the shape and the depth of soil layer and the technology of construction process [9], [10]. In the case of arch-shaped shell, the rise usually does not decrease to zero value. It remains in the structure as a residual value, induced during the assembly stage.

There is presented an example of the deformation of a drop-shaped shell, made from the plate 200 × 55 × 7 (length × depth × thickness of the wave). The structure under consideration is a real-scale culvert built within the Nowa Ruda bypass. The basic dimensions of the cross section of the shell are: the span length $L = D/2 = 7.52$ m, height $h = 6.68$ m, the radii of the top curvature $R = L/2 = 3.76$ m and of the bottom curvature $R_d = 9.60$ m. The dimension of the shell at the top is $B = 20.0$ m, and its bottom dimension is $B_d = 40.365$ m.

The location of measurement points, such as the depth of soil backfill, is referred to the level of the foundation of the shell. The in-situ measurements were taken repeatedly during the backfilling of successive layers of soil. They were carried out with the help of specialized surveying instruments. Measurement of displacements concerned:

- rise w, which is treated as the displacement of the shell at its top,
- narrowing $2u$, which is measured at a depth of $z_1 = 2.92$ m (the change of the span L);
- narrowing $2s$, which is measured as the vertical displacement at a height of $z_2 = 5.00$ m.

The values of the measured displacements w, $2u$, $2s$ shown in figure 2 are similar when the level of backfilling is about 2/3 of the depth of the shell. A considerable increase in displacements can be noticed before the backsoil reaches the level of the top of shell and the extreme values of w and $2u$ are when $z_g = h$.

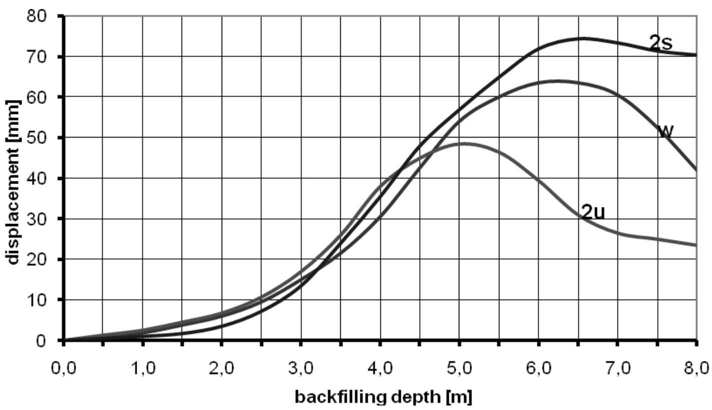

Fig. 2. Course of the rise and narrowing of shell as a function of the depth of backfill

Maximal value of narrowing $2u$ is obtained when the backsoil reaches the level of $z_g = 5.0$ m. The maximum narrowing $2s$ occurs in the same situation as the rise, i.e., in the case of $z_g = h = 6.50$ m. When the backfill is compacted above the top of the shell, all figures tend to decrease. The presented results have similar course to those obtained in other research works, e.g., [4], [9], [10]. The shapes of the plot given in figures 2 and 3 are typical of elliptic arch-shaped structures.

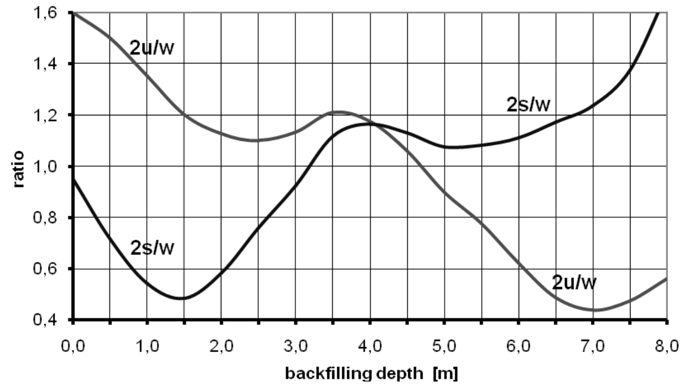

Fig. 3. Ratio of the rise and narrowing as a function of the depth of backfill

In table 1, the ratios of the rise (w/L) are presented for selected arch-shaped shells [9], [10]. The results are varied, i.e., minimal values are obtained only for the case of shell with the minimal and maximal span length L. The ratio $w/L > 1.0\%$ occurs for the shell of great depth h. The influence of strengthening plate is analysed in figure 5.

Table 1

Examples of the rise ratios of shells

Shape of shell		Arch with single radius		Arch with profile		Elliptic shell	
				high	low	horizontal	drop shape
Parameters	w/L [%]	0.30	1.42	1.95	0.30	1.53	0.86
	L [m]	2.50	11.80	9.50	20.0	10.79	7.52
	h/L	0.500	0.408	0.579	0.371	0.661	0.888
	Type of plate	100 ×20×2.5	250 ×50×5^2	150 ×50×7	380 ×140×7.1^2	200 ×55×7	200 ×55×7
	Construction site	IBDiM	Mesa	Biernacice	Gajec	Dovre	Nowa Ruda

Index (^{2}) designates the strengthening plates.

In works [3], [10], there are given the formulas which could be applied to the calculation of characteristic deflections of shell at its top, which are called the rise. To this end, the global stiffness of the soil-steel bridge must be utilized, which is determined by the ratio [3], [9], [10].

$$\lambda = \frac{E_g}{E}\frac{a}{I}L^3 \tag{1}$$

where:

E_g/E – the ratio of elasticity modules of soil and shell;

I/a – the moment of inertia of circumferential strip of shell with reference to its length a;

L – the span of shell.

However, λ does not take into consideration the basic characteristics of bridge such as the shape of a shell (closed, boxed, parabolic section, etc.), the depth of a shell and its radius of curvature, etc.

Based on the research conducted by Duncan [3], and other investigations available in literature, the following formula can be applied to the calculations of the rise [3], [9], [10]

$$w = \frac{K_w}{10^5} \frac{\gamma_g \cdot a}{EI} L^5 . \tag{2}$$

The rise w depends on the length L and linearly on the volume weight of soil γ_g and the stiffness of circumferential strip of shell EI/a. In the modified function of $K_w(\kappa, \lambda)$ with reference to the given in [3] and shown in figure 4 (in the form of a plot), the shape of shell is taken into account in the following parameter

$$\kappa = \frac{h_k}{L} . \tag{3}$$

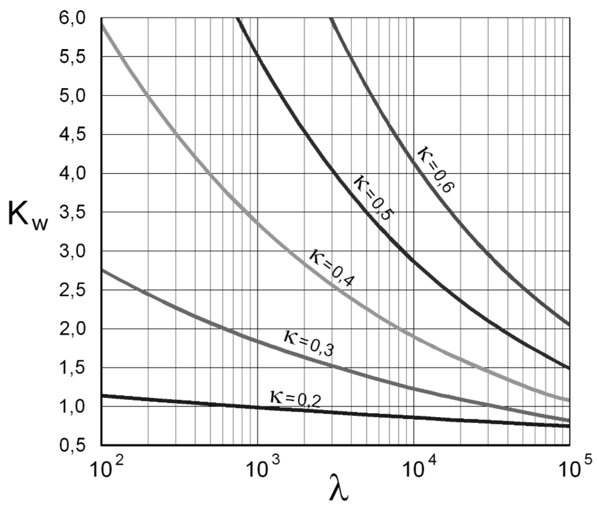

Fig. 4. The plot of the function $K_w(\kappa, \lambda)$

For the arch-shaped shell with low profile, one has $h_k = h$. Equations (1) and (2) can also be used to calculate the rise ratio

$$\frac{w}{L} = \frac{\lambda \cdot K_w}{1000} \frac{\gamma_g}{E_g} L \, [\%] \,, \tag{4}$$

which is also taken advantage of as the parameter that characterizes the stiffness of structure during backfilling.

In the steel shell characterized by large spans or low/high profile, the strengthening plates are used which are joined with the main shell. Their application results in a double increase in the area of section of the shell and about eight-fold increase in the moment of inertia of the shell section. Whenever the strengthening of the main shell is not necessary, such additional plates are applied only in some chosen waves. In figure 5, the effect of applying strengthening plate is presented in the form of plots of the calculated ratio of rise *w*/*L* as a function of span *L* of the shell.

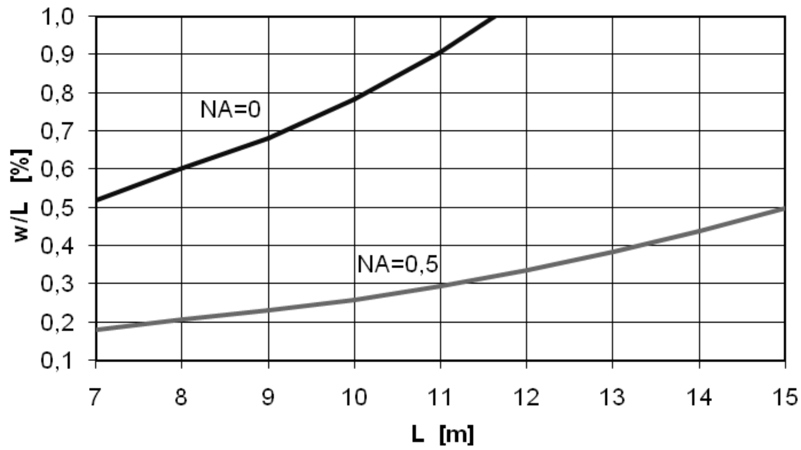

Fig. 5. Change of the ratio of the narrowing in relation to the span of shell

A parabolic-shaped shell of height h = 5 m, made of the corrugated plate 200 × 55 × 5.5 and soil backfill with the volume weight γ_g = 21 kN/m^3 and the module of elasticity E_g = 21 MN/m^2 is considered. Two results of calculations according to u are presented for the shell without additional strengthening plate NA = 0 and with additional strengthening plate fastened to the corrugated plate of the shell every second wave NA = 0.5. As can be seen from the diagram, the strengthening plate effectively limits the rise of the shell up to ca. four times due to an increase in the bending stiffness of section.

The narrowing as a horizontal displacement of the lateral walls of the structure is in general very difficult to calculate due to the variety of the shell shapes. Mostly, the shell is made out of a few segments – sheets of circular arches. The technology of lying down backfill as the process of compaction of the surrounding soil with the mechanical equipment can influence the deformation of cress section of shell. It is the effect which is not taken into consideration in calculations.

The effect of rise of the shell during backfilling is a positive phenomenon. During service life, as a result of traffic loading on the road, the shell deflects (horizontal displacement), which causes a reduction of the rise. The reduction of the deflection value is at the same time the result of the decrease in bending moments. This leads to an increase in the safety of structure, because in such a way the main component of normal stress in steel shell caused by the bending is reduced. In structures constructed as a closed box (framed) the rise phenomenon is very limited [10]. In that respect the box shell belongs to another category than the arch-shaped shells.

3. RELATION BETWEEN INTERNAL FORCES AND DEFORMATION OF SHELL

The setting of internal forces in the soil-shell structure which arise during the process of backfilling is complex, even when the applied FEM models are utilized [1], [2], [4]. This is due to the fact that at this stage of construction the surrounding soil is the loose body which is subject to the large pressure of technological loading and frequently to the dynamical and sometimes impact ones [6]. The model of soil as the structural material is very complex at this stage. The additional difficulty is due to the contact layer [5], in which the interactions $p(\varphi)$ and $t(\varphi)$ arise, as shown in figure 1. A common method of measurements of normal interactions at the soil–shell contact in the real structures [8] gives the results only for some areas. For that reason, the values of internal forces and interactions on the circumferential strip point out their random character and their large discrepancy.

In this paper, a hybrid (mixed) solution is proposed in the form of a numerical model of shell itself given by the shape, geometrical parameters (I/a and A/a) and physical ones (E = 205 GN/m^2) of the corrugated plate. To avoid the modelling of strength parameters of soil backfilling and the additional elements such as equipment of a bridge, one can take as the input data the deformation of shell, which are obtained from the in situ tests of the structure under construction. These are virtual boundary conditions for a shell structure in the form of real displacements at the selected points on the circumferential strip, as in figure 6. Virtual supports can be single (with normal directions to the shell) or double, or even mixed systems. Usually, one can obtain a linear displacement in orthogonal coordinate system from the in-situ geodetic measurements. Because of the difficulty in measuring angles of rotation of a bi-directionally corrugated plate, the moments supports are not used. To model the deformation of a shell, the circumferential strip located in the central part of the structure is usually taken into consideration. The deformation of the shell on the portals of the tunnel structure depends on a variety of factors, e.g., concrete crown, the angle and the strengthening of a slope.

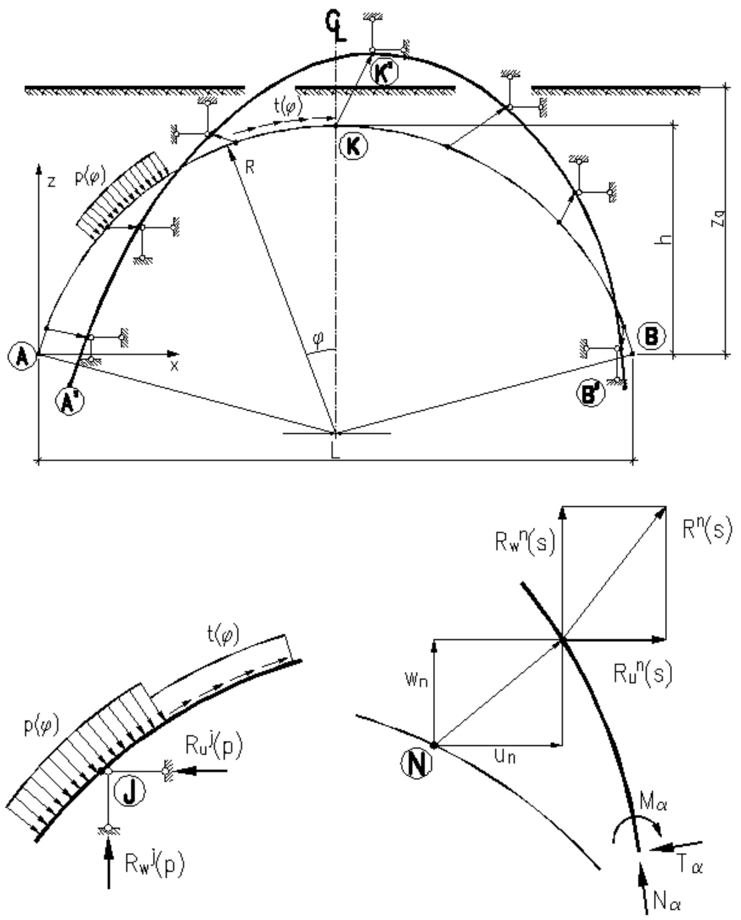

Fig. 6. Computational model of circumferential strip with virtual supports

The assumption made on the calculation model as shown in figure 6 leads to the reduction of the range of the influence of interactions $p(\varphi)$ and $t(\varphi)$ on the internal forces in the shell. These interactions are used only to the solution of a local problem, in principle to the segment between points with virtual supports, if a large number of regularly distributed virtual supports are applied. The values of measured displacements in the direction of virtual supports are here of great significance. In the paper, the main focus is on the normal interaction forces between the soil and the shell $p(\varphi)$ and on bending moments $M(\varphi)$. The bending moments $M(\varphi)$ with axial forces $N(\varphi)$ creates small eccentrics, calculated as $M/N < f$ (the height of the wave of shell).

The algorithms described can be grouped into two separate computational models. In one model, one can calculate internal forces, which are affected by $p(\varphi)$ and $t(\varphi)$ on the assumption of non-flexible virtual supports. In the second one, only imposed displacement s are taken into consideration. Summation of the results from both models leads to the same results as in the case where interactions $p(\varphi)$ and $t(\varphi)$ and displacements of measurement points s are simultaneously taken into account. On condition of the conformity of reaction in virtual supports, which are derived as the results of the displacements of nodes $R(s)$ and the load from the reaction of soil $R(p)$, as in figure 6, the intensity of interactions of $p(\varphi)$ and $t(\varphi)$ is calculated because $R(s) \approx R(p)$. The methodology of calculation is given in the exemplifying comparative analysis.

4. COMPARATIVE ANALYSIS

A bridge built over the stream of Piekielnica on the Nowa Ruda bypass is taken as a sample bridge in the analysis. The geometrical parameters of the bridge are: span $L = 13.50$ m, the height of arch-shaped shell $h = 5.006$ m, the type of corrugated plate $380 \times 140 \times 7.1$. There are two arches in the circumferential strip: one with radius $R = 9.930$ m in the top part, and $R_n = 3.430$ m at the haunch, the respective angles being $\varphi_R = 61.52°$ and $\varphi_{Rn} = 70.45°$. In the calculations, a symmetric shape of the circumferential strip deformations was assumed, which enabled us to analyse half structures only with a circumferential strip $a = 1.0$ m. Both arches (of radius R and R_n) were approximated numerically with ten finite beam elements. The shell's geometry is shown in figure 7.

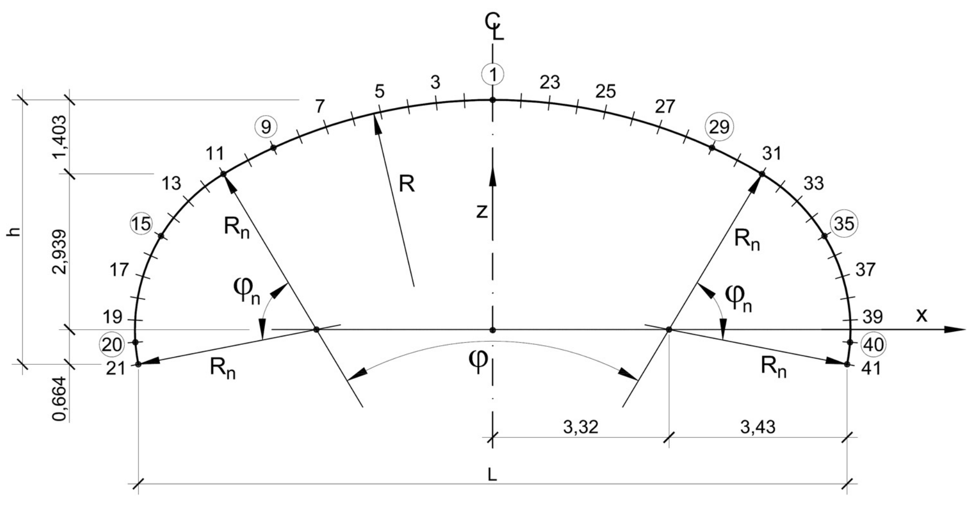

Fig. 7. Static scheme of the structure under consideration

With the aim of comparison, the results of calculations in the case of assumed loading $p(\varphi)$, uniformly distributed along the length of elements analyzed and the intensity given in table 2 are taken as the exact solution. The distribution of interaction between soil and the shell $p(\varphi)$ corresponds to the level of backfill 0.7 m above the top of the shell, i.e., $z_g = 0.70 + h$. In the calculations, the tangent component of interaction $t(\varphi)$ was neglected. The assumed model of the static scheme without virtual supports was taken into consideration. The displacements obtained from these calculations, given in table 2, are treated in numerical simulation as the results of in situ measurements. All the results, displacements and internal forces obtained from the model M0, without virtual supports, are accurate results. Displacements obtained from the calculations, given in table 2, are treated in numerical simulation as the results of accurate and precise in-situ geodetic measurement.

Table 2

Data for the numerical simulation

No of node or element	Loading of shell elements $p(\varphi)$ [kN/m^2]	Displacements of node (mm)	
		w	u
1	15.1	33.4875	0
2	16.1	32.5859	0.0931
3	17.1	29.9739	0.3660
4	21.1	25.9201	0.9628
5	25.1	20.8459	1.9611
6	29.1	15.2769	3.3508
7	34.1	9.7739	5.0299
8	40.1	4.8623	6.8172
9	42.1	0.9605	8.4836
10	47.1	–1.6949	9.8066
11	56.1	–3.0958	10.6329
12	65.1	–3.4434	10.9311
13	68.1	–3.2146	10.8250
14	75.0	–2.6521	10.303
15	75.0	–1.9438	9.4793
16	75.1	–1.2243	8.3168
17	75.1	–0.5942	6.9040
18	75.1	–0.1231	5.3085
19	75.1	0.1464	3.5938
20	75.1	0.1914	1.8124
21	support	0	0

In models M2–M6, the boundary conditions are measured displacements (calculated in model M0). The variable parameter of analysis is the number of points in which the displacements are determined: M2 – two points, M6 – six points (taking into account the symmetry of deformation), given in table 3. In view of these assumptions, the common features of models M0 and M2–M6 are the geometry and stiffness of the shell. Internal forces in the shell are calculated on the basis of completely different boundary conditions. They are used in estimation of the accuracy of results derived from the approximate models M2–M6.

Table 3

Results from numerical simulation

Models	M6	M5	M4	M3	M2
Virtual supports at nodes	1, 4, 7, 10, 13, 16	1, 5, 9, 13, 17	1, 6, 11, 16	1, 7, 13	1, 11
$M_k(s)$ [kNm]	30.684	28.858	26.653	24.285	31.565
m	0.913	0.859	0.793	0.723	0.939

As the criterion of usability of those models, the value of bending moment at the top section of the shell (maximum value of bending moments in the circumferential strip) is assumed. The example of simulation (calculations) results in the form of bending moments, as given in fig. 8a, was obtained only from the deformations of the shell, determined on the basis of displacements of points given in table 2 and virtual supports of models in table 3. The values of moments at the top of the shell $M_k(s)$ which arose from the imposed displacements are listed in table 3 and compared with $M_k(p)$ = 33.603 kNm, which was obtained as the results of assumed loading $p(\varphi)$ in model M0.

$$m = \frac{M_k(s)}{M_k(p)} . \tag{5}$$

Model M2, in which the displacements of only two characteristic points as in figure 1 describe the rise and narrowing, gives a very good approximation of the exact graph (as in figure 8a). This is not coincidence but regularity in the representation of the deformation of shell during backfill compaction process. This justifies the investigation of the ratio w/u, shown in figure 3, with reference to the different shapes of shell.

The significant values of bending moments in the lateral area of shell shown in fig. 8b can be treated as the result of simplification in the applied computational model. Higher accuracy of the results can be obtained after taking into consideration the estimated load $p(\varphi)$. By means of the conformity conditions of the reaction forces in virtual supports, as in fig. 6, one can obtain:

$$R_u^i(s) = R_u^i(p) \tag{6}$$

and

$$R_w^i(s) = R_w^i(p) . \tag{7}$$

a)

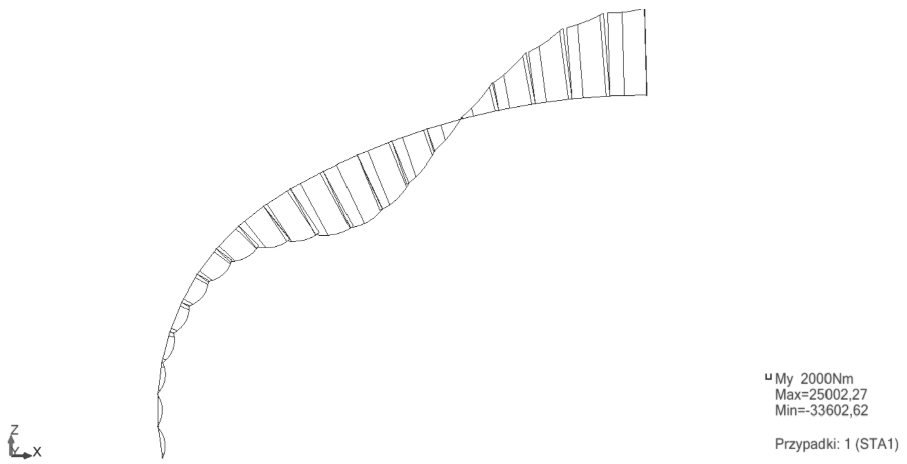

b)

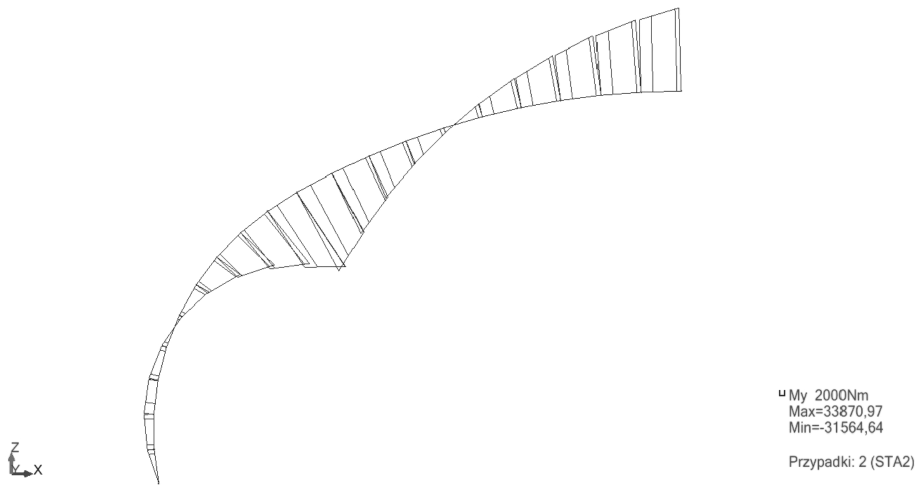

Fig. 8. Bending moment diagram in the shell due to
a) the reaction of the soil, b) the displacements imposed in model M2

Reactions $R(s)$ can be used for the calculations of the reaction of soil on the shell $p(s)$, designated in figure 1 as $p(\varphi)$. In the case of dense arrangements of virtual supports (measurement points) located on the circumferential strip of shell, the approximation shown in figure 9 is sufficient in the form of:

$$p(s) = \frac{R_n}{a} \tag{8}$$

and

$$t(s) = \frac{R_t}{a} \tag{9}$$

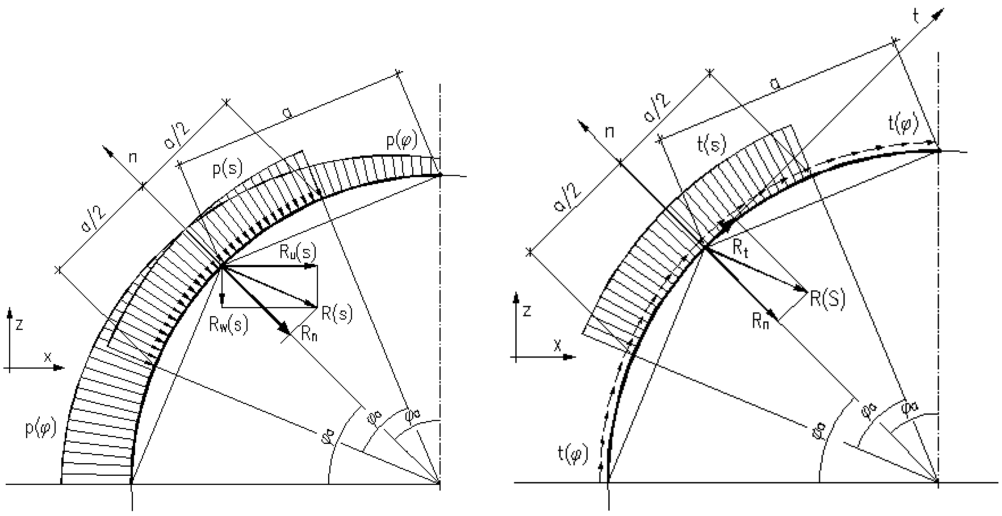

Fig. 9. Approximation of the soil–shell interaction

Table 4

Results of the calculations of soil–shell interactions $p(s)$ [kN/m^2]

Model	No. of virtual supports	Length of chord a [m]	Components of reaction in virtual supports [kN]			Interaction force $p(s)$ [kN/m^2]	Accuracy n
			R	R_u	R_w		
M6	1	1.565	22.800	–	22.80	14.57	0.965
	4	1.565	29.317	7.43	28.36	18.73	0.888
	7	1.565	49.498	22.10	44.29	31.63	0.928
	10	1.565	66.151	36.65	55.07	42.27	0.897
	13	1.452	79.820	57.40	55.47	54.97	0.807
	16	1.338	84.896	69.31	56.35	63.45	0.845
M5	1	2.091	28.600	–	28.60	13.68	0.906
	5	2.091	50.084	32.13	38.42	23.95	0.954
	9	2.091	77.109	51.31	57.56	36.88	0.876
	13	1.910	90.655	75.62	50.00	47.46	0.687
	17	1.784	104.49	99.90	30.64	58.57	0.780
M4	1	2.611	33.101	–	33.10	12.68	0.840
	6	2.611	97.502	90.88	35.32	37.34	1.283
	11	2.611	83.928	59.73	58.96	32.14	0.621
	16	2.206	97.017	91.73	31.59	43.98	0.586

Table 4 contains the results of calculations of normal components of reaction of the backfill on the shell $p(s)$ based on virtual supports which are applied in the calculation model to represent the displacements of the shell. The values of $p(s)$ are the forces distributed over the length of the chord of arch a between measurement points. In this case, the value of normal reaction to shell $R_n(s)$ is calculated as the resultant using the formula:

$$R_n \approx \sqrt{R_u^2(s) + R_w^2(s)} \ . \tag{10}$$

Comparing the calculated soil–shell interaction forces, $p(s)$, with regard to $p(\varphi)$, given in table 2,

$$n = \frac{p(s)}{p(\varphi)} \tag{11}$$

can be recognized as technically satisfactory. Considering the value of n it is clear that the larger number of measurement points enables a more accurate modeling of soil interaction $p(s)$. Models M3 and M2 are not useful in such calculations.

Taking into account the additional loading of shell $p(s)$ in the models under consideration M6–M4, the accuracy of results is improved. This is due to the fact that the overall result of calculations consists of the part caused by the imposed displacements, $M(s)$, and the part caused by the loading of the shell $M(p)$, calculated in the model with virtual supports. An example of such results for model M5 is presented in figure 10. The corrected graph of bending moments is similar to the exact result, as shown in fig. 8a.

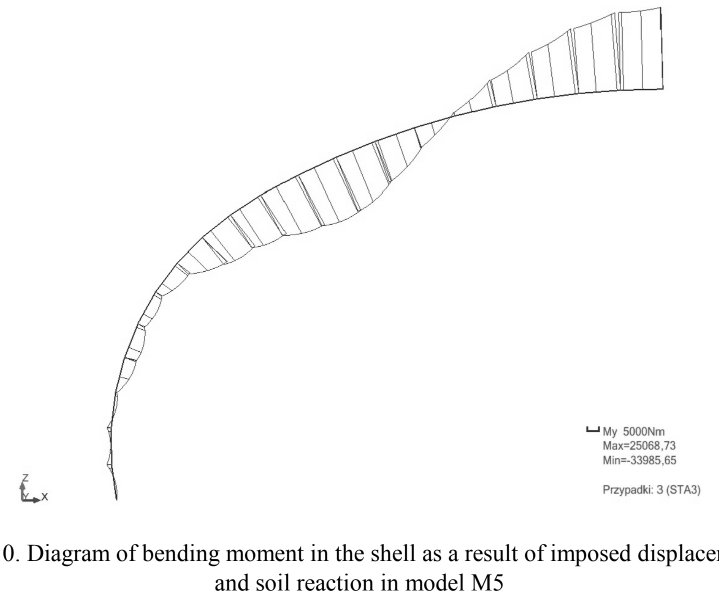

Fig. 10. Diagram of bending moment in the shell as a result of imposed displacements and soil reaction in model M5

5. INTERNAL FORCES IN THE STEEL SHELL OF REAL BRIDGE

In the case of modelling the deformation of real soil-steel shell structure, one does not use the design support conditions because of the fact that the shell–support contact layer does not need to be effective. The foundation of bridge can settle during the construction phase. Based on the example deformations of shell determined by in situ tests, see figure 6, one can conclude that the points of support on foundation A and B were relocated to positions A′ and B′. Thus, this support reaction is not determined due the fact that the shell is in a way hanged in the soil. In order to guarantee the static equilibrium conditions, the virtual supports and the values of displacements in these directions, shown in figure 6, are sufficient.

Table 5

Results of the measurements of shell displacements

Displacements	Number of shell nodes						
	19	15	9	1	29	35	39
w [mm]	–10	–10	–4	47	–7	–15	–14
u [mm]	13	14	10	10	–18	–18	–11

As an example of calculations of the effects of measured displacements of steel plate in real structure, the bridge analyzed in section 4 is again under consideration. The construction stage when the depth of backfilling soil is at the level of the top of the shell, i.e., when $z_g = h = 5$ m and the rise reaches its maximum value is considered. On account of the large values of displacements of the shell given in table 5 it was possible to apply precise geodetic measurements.

From the calculated deformation presented in figure 11a one can see the zones of characteristic displacements: the rise and the narrowing. No extreme values of displacements have appeared at the point of measurements (point 1 – the top):

$$s_1 = \sqrt{47^2 + 10^2} = 48.05 \text{ mm}$$

but at the point 24

$$s_{24} = \sqrt{76.92^2 + 10.91^2} = 87.60 \text{ mm}$$

being larger by ca. 82.5%. The plot of bending moments presented in figure 11b points to the accuracy of the extreme values M_{24} = 163.67 kNm, a couple of times larger than calculated at the axis of symmetry (at the top) $M_k = M_1$ = 47.72 kNm. The lack of symmetry of displacements and internal forces is obviously the result of the technology of compaction of back soil on the structure.

a)

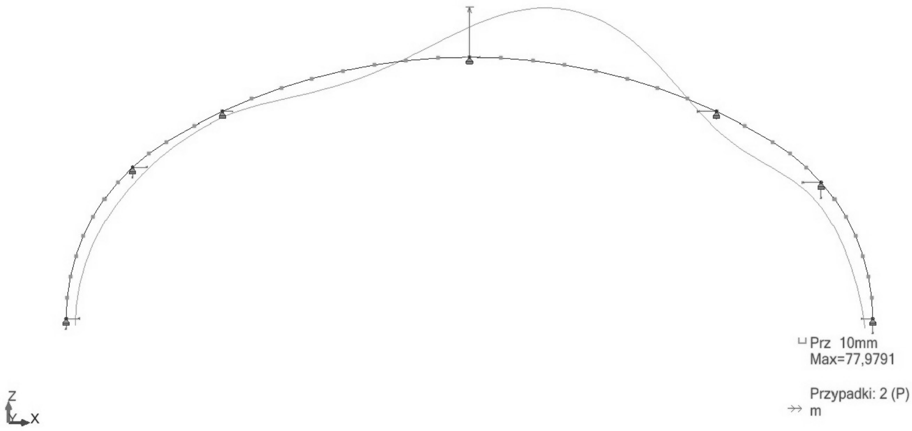

b)

Fig. 11. Deformation of the shell and diagram of bending moments in the shell due to measured displacements

The presented results of calculations show the efficiency of the determination method of deformations and extreme values of displacements based on measurements. At the chosen points of the shell, the shape of its deformation can be considered in the determination of bending moments and particularly, its maximal value. A simple computational FEM model with the use of beam elements [10] can be employed for this task. The influence of construction technology on the deformation of shell and internal forces is significant. The values of axial forces in the shell are of the same sign and their course is monotonic. The modeling of the value of axial forces is well known, e.g. [10], and thus it is not raised in the paper.

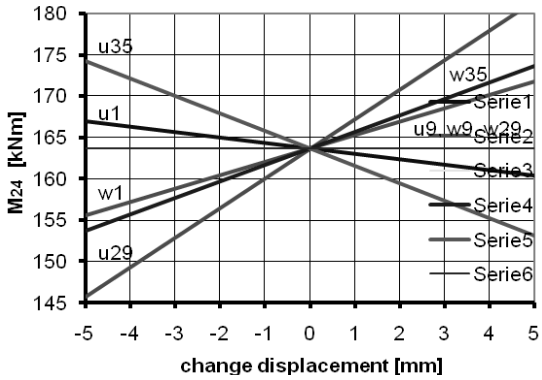

Fig. 12. Estimating the sensitivity of a solution

In the case of any algorithm being formulated, the estimation of the sensitivity of solution is of great importance. In the paper, the maximum value of bending moment at the top of the arch M_{24} as a function of the change of displacements in the direction of virtual support is considered. The variables are taken as single displacements of virtual supports, neglecting the modification of the location of remaining supports. In figure 11, the results of calculations are given. Deviations from the mean values of the displacements analyzed, as listed in table 5, are shown on the horizontal axis and on the vertical axis the values of M_k are given. The graphs presented in figure 11 are assumed to be linear. One can see the satisfactory sensitivity of solution from the diagrams shown in these figures. Even some significant deviation of the measured displacements ±5 mm, taken in calculations, compared with the measured displacements, does not lead to any significant change in the bending moment M_{24}, because $\Delta M_{24} = \pm 18$ kNm/m., which is ca. 11%. This proves the possibility of applying precise geodetic measurement results.

An increase in the accuracy of modelling the deformation of structure and internal forces is obtained after addition operation of the results derived from displacements and other results from the soil–shell interaction – in the model with virtual supports. Then the local extreme values of bending moments shown in figure 11 are reduced, in the lateral areas of shell.

6. SUMMARY

The work is concerned with the soil–steel culverts made of arch-shaped steel corrugated plates. The modelling of deformation of this type of structure during their construction stage by means of general FEM based computation system despite the large availability of examples proved to be difficult on account of the complex characteristics soil medium assumed the loose body and the significant influence of the construction technology. In the paper, there is proposed the methodology for the estimation of characteristic displacements of the steel shell which is the phenomenon of the rise determined on the basis of measurement results of constructed structures. On the example of the constructed culvert, the course of shell deformation during the process of backfilling of the bridge and the relation between the displacements of characteristic points of the shell is presented.

The advantage of the algorithm proposed which enables us to determine deformation and internal forces in the shell on the basis of measurement results at its chosen points lies in the simplification and reduction of the computational model to the analysis of steel shell only – the element of the structure characterized by the elastic physical parameters and precisely determined geometrical characteristics (corrugated plate). Such a computational model makes is possible to estimate the technological effects during construction stage and to estimate changes in the physical characteristics of soil medium during the process. By the example of calculations of the constructed bridge, the feasibility of the algorithm proposed and the possibility of applying geodetic techniques to the measurement of displacements have been proved.

The measurements of displacements can concern any stage of service life. The application of virtual boundary conditions for the shell in the form of measured displacements on the real bridge enables one to improve the accuracy of the modelling of deformations and internal forces in the corrugated shell of steel structure. These effects are certainly taken into consideration in the displacement of additional supports of steel shell.

REFERENCES

[1] MOORE J.D., TALEB B., *Metal Culvert Response to Live Loading Performance of Three-Dimensional Analysis*, 78th Annual Meeting of the Transportation Research Board, Washington, D.C., 1999.

[2] TALEB B., MOORE J.D., *Metal Culvert Response to Earth Loading Performance of Two-Dimensional Analysis*, 78th Annual Meeting of the Transportation Research Board, Washington, D.C., 1999.

[3] DUNCAN J.M., *Behaviour and design of long span metal culverts*, Journal of Geotechnical Engineering Division ASCE, GT3, 1979, 399–418.

[4] SEED R.B., OU CHANG-YU., *Measurements and Analyses of Compaction Effects on a Long-Span Culvert*, Transportation Research Record 1087.

[5] KATONA M.G., *A simple contact-friction interface element with application to buried culverts*, Proc. of Symp. Implementation of Computer Procedures and Stress-Strain Laws in Geomechanical Engineering, Chicago, Illinois, 3–6 August 1981, 45–63.

[6] MACHELSKI CZ., ANTONISZYN G., MICHALSKI B., *Influence of Live load on the Soil-steel Bridge Founded on Elastic Supports*, Studia Geotechnica et Mechanica, 2006, 2–4, 65–82.

[7] MACHELSKI CZ., ANTONISZYN G., *Influence of live load on the soil-steel bridges*, Studia Geotechnica et Mechanica, 2004, 3–4, 91–119.

[8] VASLESTAD J., *Soil structure interaction of buried culverts*, Institutt for Geoteknikk, Norges Tekniske Hogskole, Universitetet I Trondheim, 1990.
[9] MACHELSKI CZ., MICHALSKI J.B., JANUSZ L., *Deformation Factors of Buried Corrugated Structures*, Transportation Research Board, Washington, 11–15 January 2009, (09–1796).
[10] MACHELSKI Cz., *Modelowanie mostowych konstrukcji gruntowo-powokowych*, Dolnośląskie Wydawnictwo Edukacyjne, Wrocław, 2008.
[11] MOHAMEDZEIN Y.E.-A., CHAMEAU J.L., *Elastic Plastic Finite Elemente Analysis of Soil-Culvert Interaction*, Sudan Engineering Sociaty Journal, January 1997, Vol. 43, No. 34, 16–29.